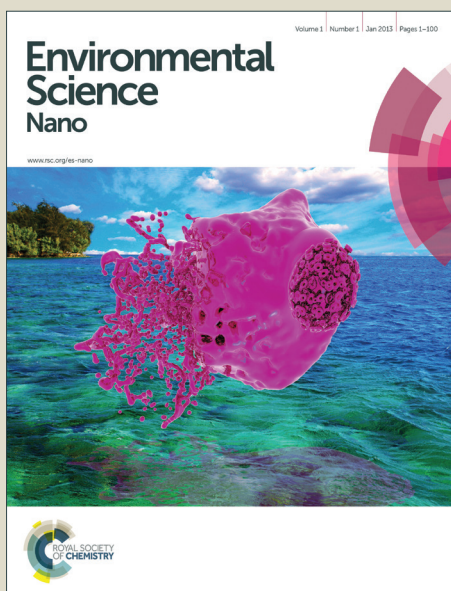


# Environmental Science Nano

Accepted Manuscript



This is an *Accepted Manuscript*, which has been through the Royal Society of Chemistry peer review process and has been accepted for publication.

*Accepted Manuscripts* are published online shortly after acceptance, before technical editing, formatting and proof reading. Using this free service, authors can make their results available to the community, in citable form, before we publish the edited article. We will replace this *Accepted Manuscript* with the edited and formatted *Advance Article* as soon as it is available.

You can find more information about *Accepted Manuscripts* in the [Information for Authors](#).

Please note that technical editing may introduce minor changes to the text and/or graphics, which may alter content. The journal's standard [Terms & Conditions](#) and the [Ethical guidelines](#) still apply. In no event shall the Royal Society of Chemistry be held responsible for any errors or omissions in this *Accepted Manuscript* or any consequences arising from the use of any information it contains.

Nanomedicine is a rapidly advancing field in preclinical research, but successful clinical outcomes are still limited. It is important to better understand some of the shortcomings of nanoparticles including changes in intrinsic toxicity to nanomaterials due to their unique size. Carbon nanotubes have been investigated as drug delivery vehicles and imaging agents, but limited research has been performed on their toxicity. In this study we investigate whether MWCNTs can cause toxicity from desorbed polyaromatic hydrocarbons and compare potential toxicity with carbon black.

Revised and resubmitted to Environmental Science: Nano

final

1                                   **Carbon Nanomaterials Rescue Phenanthrene Toxicity**  
2                                   **in Zebrafish Embryo Cultures**

3  
4                                   Jonathan L. Falconer<sup>1</sup>, Clinton F. Jones<sup>1</sup>, Shan Lu<sup>2</sup>, David W. Grainger<sup>1,2,3</sup>

5  
6                                   <sup>1</sup>Department of Pharmaceutics and Pharmaceutical Chemistry, Health Sciences, University of  
7 Utah, Salt Lake City, UT 84112-5820 USA

8                                   <sup>2</sup>Department of Bioengineering, University of Utah, Salt Lake City, UT 84112 USA

9                                   <sup>3</sup>Utah Center for Nanomedicine, Nano Institute of Utah, University of Utah, Salt Lake City, UT  
10 84108 USA

11  
12  
13  
14  
15                                   **Corresponding Author**

16                                   David W. Grainger, Ph.D.

17                                   Department of Pharmaceutics and Pharmaceutical Chemistry

18                                   University of Utah

19                                   Salt Lake City, UT 84112-5820 USA

20                                   Email: david.grainger@utah.edu

21                                   Tel: 801-581-3715

22                                   Fax: 801-581-3674

23  
24  
25  
26                                   Keywords: carbon nanotube, carbon black, polyaromatic hydrocarbon, adsorption, phenanthrene

## 30 **Abstract**

31 Multi-Walled Carbon Nanotubes (MWCNTs) and Carbon Blacks (CB) are known to carry wide  
32 varieties of adsorbed, potentially toxic chemicals resulting from their manufacturing, typically  
33 including metals and polyaromatic hydrocarbons (PAHs). Instead of desorption of these  
34 adsorbates into aqueous milieu, substantial high-affinity adsorption of the aqueous dispersed  
35 PAH, phenanthrene to MWCNTs and CB from aqueous solutions and dispersions is reported.  
36 Phenanthrene adsorption to aqueous dispersed carbon nanomaterials phases was measured  
37 using isotherms and then exploited to remove toxic levels of phenanthrene from aqueous media  
38 incubating zebrafish embryos (ZFEs) as a whole organism toxicity screening system.  
39 Remarkable reduction in phenanthrene-induced ZFE toxicity was observed using two  
40 experiments: one comparing PAH concentration-dependent rescue of ZFE viability from  
41 MWCNTs compared to carbon black (CB), and a second examining kinetics of the ZFE rescue by  
42 MWCNTs vs. CB incubations after initial ZFE exposure to phenanthrene for 2 hours.  
43 Phenanthrene LD<sub>50</sub> concentration in the absence of any carbon-based sorbent increases  
44 dramatically to 10 µg/ml in the presence of either 81.3 µg/ml MWCNTs or 81.5 µg/ml CB  
45 materials. When CB and MWCNTs were added to ZFEs previously exposed to 10 µg/ml  
46 phenanthrene for 2 hours, significant rescue of ZFE viability was observed in CB-treated embryos  
47 while no ZFE rescue was observed in MWCNT-treated ZFEs. This result is consistent with an  
48 expected carbon nanomaterial surface area-dependent ZFE rescue effect: CB exhibits a higher  
49 Brunauer-Emmett-Teller (BET) surface area than the MWCNTs used, with higher adsorption  
50 capacity likely for phenanthrene, yielding ZFE rescue from toxicity.

51

## 52 **Introduction**

53 Use of carbon nanotubes (CNTs) in both consumer and medical products has increased  
54 dramatically over the past decade and continues to increase.<sup>1</sup> Their broadening applications  
55 significantly raise the potential for human exposure to CNTs by various uncontrolled, inadvertent

56 (i.e., unintentional environmental and occupational exposure) and controlled, deliberate (i.e.,  
57 biomedical imaging, drug delivery exposure) routes and dosings. This has implications for human  
58 toxicity risks with these carbon-based nanomaterials. Recent findings suggest a variety of  
59 material architecture-dependent CNT toxicological effects ranging from asbestosis-like responses  
60 to some inhaled single-walled CNTs (SWNTs)<sup>2</sup> to increased inflammation when multi-walled  
61 carbon nanotubes (MWCNTs) are exposed to the epidermis.<sup>3</sup> Beyond intrinsic CNT toxicity  
62 mechanisms, another major concern is the potential for CNTs, with their high specific surface  
63 areas (200-800 m<sup>2</sup>/g),<sup>4</sup> known levels of contamination from their manufacture,<sup>5</sup> and lack of  
64 adequate surface characterization in many reports<sup>6</sup> to carry both adsorbed heavy metal catalysts  
65 used in CNT production and adsorbed polyaromatic hydrocarbons (PAHs) as by-products of CNT  
66 manufacture<sup>7</sup> and other adsorbed ubiquitous environmental contaminants.<sup>6, 8</sup> These “loadings” of  
67 contaminants on CNT surfaces can constitute considerable adsorbate dosing to living systems  
68 under reasonable CNT particle exposures.<sup>6</sup> However, CNT-PAH adsorption is likely stabilized on  
69 CNT surfaces by hydrophobic  $\pi$ -stacking binding affinities comparable in energetics to hydrogen  
70 bonds.<sup>5, 9</sup> Therefore, “delivery” of such adsorbates into biological systems and their resulting  
71 dosing and bioavailability from CNT exposure is currently unknown. In many biological milieus,  
72 CNT transport into lipid microenvironments (e.g., cell membranes, chylomicrons) and interactions  
73 with globular proteins (e.g., albumin, lipoproteins) could facilitate or promote desorption of CNT-  
74 associated PAHs into host tissues with possible toxicological implications.

75  
76 The effects of CNT-PAH exposure in the whole-organism zebrafish embryo (ZFE) toxicity model<sup>10</sup>  
77 were studied here using phenanthrene (a 3-ring PAH) as a model toxin and adsorbate.  
78 Phenanthrene was chosen as a model PAH due to its suspected high adsorptive capacity to  
79 MWCNT and finite solubility in 1% DMSO aqueous milieu. The working hypothesis was that ZFE  
80 toxicity induced by PAHs in solution would be mitigated by high surface-area carbonaceous  
81 nanoparticle adsorbents. MWCNTs were added to ZFEs in 1% DMSO to observe intrinsic

82 MWCNT toxicity and associated toxicity from desorbed species. Previous studies have  
83 demonstrated that 1% DMSO exhibits no observable adverse biological effects.<sup>11</sup>

84  
85 Carbon black (CB) - well-known as a clinically useful and safe sorbent for various organic  
86 compounds<sup>12</sup>- was selected for comparison to MWCNTs in this model. Experiments determined  
87 phenanthrene toxicities in the ZFE model, then monitored ZFE toxicity under different PAH  
88 exposures with carbon nanomaterials in ZFE media to determine LD<sub>50</sub> and LD<sub>90</sub> values.  
89 Phenanthrene concentration in both absence and presence of MWCNTs provided PAH  
90 adsorption/desorption isothermal analysis with added MWCNTs. Varying ratios of MWCNTs and  
91 CBs in the presence of fixed toxic concentrations (LD<sub>90</sub> = 10µg/ml) of phenanthrene were  
92 assessed after two hours of ZFE pre-exposure to phenanthrene. ZFE viability was then assessed  
93 as a function of PAH exposure.

94

## 95 **Materials and Methods**

96 *Chemicals and sample preparation:* phenanthrene (Acros Organics, >97%) and dimethyl  
97 sulfoxide (DMSO, HPLC grade, Fisher, USA) were used as supplied. Cleaned multi-walled  
98 carbon nanotubes (MWCNT, BuckyUSA) were described as 95% pure by the manufacturer with a  
99 diameter of 5-15 nm and a length of 1-10 µm. Mass spectrometric analysis (ICP-MS) was  
100 performed on MWCNTs digested in nitric acid, and concentrations of 42 elemental impurities  
101 were measured. Nonporous carbon black (CB, Cabot, USA) was classified as a high-purity  
102 furnace black with low amounts of total PAHs (<0.5 ppm). Carbon Black was also analyzed by the  
103 identical ICP-MS method. Phenanthrene was dissolved in DMSO at a stock concentration of 1  
104 mg/ml which was then diluted 1:100 in Millipore-polished ASTM grade 1 water to yield a final  
105 concentration of 10 µg/ml phenanthrene in 1% DMSO aqueous dispersion as a stock solution.  
106 Phenanthrene was stored in the dark to avoid photodegradation. Similar separate stock solutions  
107 of 2 mg/ml CB and MWCNTs in 1% DMSO were also prepared.

108  
109 *Zebrafish embryo (ZFE) exposures:* Adult wild-type AB zebrafish (*Danio rerio*) were bred and  
110 maintained using standard procedures.<sup>13</sup> All zebrafish experiments were performed in compliance  
111 with institutional guidelines and approval from The Institutional Animal Care and Use Committee.  
112 Fertilized eggs were collected at 2 hours post fertilization (hpf) and rinsed in a dilute methylene  
113 blue solution. Embryos between 3-4 hpf were then added individually to a non-tissue culture 96-  
114 well plate (one embryo per well). Each experimental condition included 12 embryos (n=12) and  
115 the concentration-dependent experiment was performed four times (N=4 independent replicates)  
116 (Figure 3) and the time-dependent experiment (Figure 4) was performed in triplicate (N=3  
117 independent replicates). ZFEs were added to wells containing 90  $\mu\text{L}$  of 10  $\mu\text{g}/\text{ml}$  phenanthrene in  
118 1% DMSO in Millipore ASTM grade 1 water. Carbon nanomaterials (MWCNTs, CB) were then  
119 added in 10  $\mu\text{L}$  volumes from stock solutions to wells to reach final concentrations of 200, 100,  
120 50, or 25  $\mu\text{g}/\text{ml}$  carbon nanomaterials, 10  $\mu\text{g}/\text{ml}$  phenanthrene, and 1% DMSO in Millipore ASTM  
121 grade 1 water. This milieu was always prepared fresh immediately prior to its dosing into ZFE  
122 cultures. Embryos were treated for at least 24 hours and visualized on an M80 stereomicroscope  
123 (Leica). Positive controls comprised ZFEs in 100  $\mu\text{L}$  of 10  $\mu\text{g}/\text{ml}$  phenanthrene in 1% DMSO in  
124 Millipore ASTM grade 1 water. Negative controls comprised ZFEs in 100  $\mu\text{L}$  of 1% DMSO in  
125 Millipore ASTM grade 1 water. ZFE viability was determined by visual assessment of ZFE tissue  
126 opacity.<sup>14</sup>

127  
128 *Materials characterization:* Surface areas for MWCNTs and CB were measured by Brunauer-  
129 Emmett-Teller (BET) analysis of nitrogen physisorption at 77 K using a Micromeritics ASAP 2000  
130 instrument.<sup>15</sup>

131  
132 *Measurement of phenanthrene in solution:* Phenanthrene solution concentration was determined  
133 using UV/Vis spectrophotometry ( $\lambda_{\text{max}} = 251 \text{ nm}$ , Varian Cary 400 Biospectrophotometer 200-

134 900nm). Supernatant was removed from MWCNT/phenanthrene mixtures to measure extent of  
135 PAH adsorption as a function of varying MWCNT concentrations (100  $\mu\text{g/ml}$  and 50  $\mu\text{g/ml}$ ).  
136 Optical absorbance measurements were performed 20-40 minutes after preparing phenanthrene  
137 solutions, time sufficient to allow MWCNTs to settle from solution as evidenced by the  
138 disappearance of the MWCNT optical absorbance signature from these solutions. Settling time  
139 determined by UV/Vis spectroscopy was reflected by the lack of optical absorbance above 300  
140 nm where MWCNTs exhibit a strong characteristic absorbance, but where phenanthrene does  
141 not. Phenanthrene concentration was also measured by HPLC (Thermo Scientific Finnigan  
142 Surveyor HPLC with UV/Vis and fluorescence detection, C18 reverse-phase 100 mm x 4.6 cm  
143 column) using fluorescence detection at wavelengths of 260/380 nm excitation/emission,  
144 respectively.

145  
146 *Monitoring phenanthrene adsorption to MWCNTs:* Phenanthrene solutions (10  $\mu\text{g/ml}$ ) in 1%  
147 DMSO were prepared by adding a 1:100 dilution of 1 mg/ml phenanthrene in 100% DMSO to  
148 Millipore-polished ASTM grade 1 water. MWCNTs were dispersed in a Branson 5210 bath  
149 sonicator at maximum power for 10 minutes and then added to this PAH solution to reach a final  
150 concentration of 30, 50, 100, 150, 200, and 500  $\mu\text{g/ml}$  from a 2 mg/ml stock solution in Millipore-  
151 polished ASTM grade 1 purified water. This sonication method is previously reported to effectively  
152 disperse MWCNTs.<sup>16</sup> The mixture of MWCNTs and phenanthrene was allowed to incubate  
153 unstirred at room temperature under ambient air for 90 minutes. MWCNTs were then separated  
154 from the solution by standing and the supernatant was measured spectrophotometrically at 251  
155 nm and room temperature. Concentrations of phenanthrene were calculated by comparison to a  
156 phenanthrene standard curve generated under these same conditions. Langmuir adsorption  
157 isotherms were generated from optical absorbance data for phenanthrene solutions using open-  
158 access curve fitting software at [www.zunzun.com](http://www.zunzun.com) (last accessed June, 2014). Specifically,  
159 nonlinear regressions were fit to the Langmuir equation:  $q_e = Q^0 C_e / (K_d + C_e)$  where  $q_e$  (amount of



160 phenanthrene adsorbed per unit MWCNT) and  $C_e$  (bulk concentration of phenanthrene) are  
161 known, measured quantities.  $Q^0$  was derived from the best-fit result.

162

163 *Statistical Analysis:*

164 Statistical analysis was performed by two-tailed Dunnett's test using ANOVA provided by the  
165 XLSTAT add-in module in Microsoft Excel v.2010. Significance was defined as  $p < 0.05$ . Pairwise  
166 differences were compared between untreated 10  $\mu\text{g/ml}$  phenanthrene-treated ZFEs and 10  
167  $\mu\text{g/ml}$  phenanthrene-treated ZFEs in the presence of either MWCNTs or CB.

168

## 169 **Results**

170 MWCNTs were found to be 98.6% pure by ICP-MS analysis, with the largest impurities being  
171 nickel (0.86%) and iron (0.2%). No other non-carbon elements were present above 0.2%.  
172 Carbon Black was found to be 99.8% pure with the largest impurity being potassium (0.14%).  
173 BET analysis performed to compare the surface areas of MWCNTs and CB samples determined  
174  $138.9 \text{ m}^2/\text{g}$  for MWCNTs and  $232.9 \text{ m}^2/\text{g}$  for CB. These results agree well with previous surface  
175 area data for analogous carbon nanomaterials.<sup>17-20</sup>

176

177 Phenanthrene concentration was measured by HPLC to characterize the physical state of  
178 phenanthrene in solution. Two distinct fluorescence peaks were observed in HPLC traces (data  
179 not shown): one early-eluting sharp peak (ex 260/em 380nm) and one later-eluting broad peak  
180 (ex 260/em 380nm). The relative area under this broad peak decreased over a period of hours  
181 and at one week was undetectable (attributed to aqueous phase separation of suspended  
182 phenanthrene). In order to determine the adsorption capacity of phenanthrene on MWCNTs,  
183 phenanthrene presence in solution was analyzed by optical spectroscopy to generate adsorption  
184 isotherms for phenanthrene on MWCNTs. Absorption spectra are shown in Figure 1 with  
185 phenanthrene concentrations calculated from optical absorption peaks at 251 nm. Analogous

186 adsorption isotherm construction for CB was hindered by the greater CB aqueous dispersive  
187 properties (i.e., no sedimentation), increasing solution opacity and preventing precise optical  
188 density measurements for phenanthrene. Adsorption data were fit to a Langmuir adsorption  
189 isotherm ( $R^2=0.957$ , Figure 2).

190

191 Both exposure of ZFEs to 1% DMSO in aqueous media, or to MWCNTs or CBs at variable solid  
192 dispersed dosings in 1% DMSO aqueous dispersions (from 25 to 10,000  $\mu\text{g/ml}$ ) produced no  
193 visible ZFE toxicity or mortality. Exposure of ZFEs to aqueous phenanthrene alone (10  $\mu\text{g/ml}$ )  
194 resulted in significant toxicity and reliable mortality in 90% of embryos ( $n=96$ ,  $\text{LD}_{90}=10$   $\mu\text{g/ml}$ ).  
195 Importantly, incubation of CB or MWCNTs to phenanthrene solutions of 10  $\mu\text{g/ml}$  ZFEs  
196 significantly reduces ZFE phenanthrene-induced toxicity (Figure 3). This is observed to be  
197 carbon nanomaterial dose-dependent, an effect akin to ZFE “rescue” from PAH-induced toxicity.  
198 ZFE rescue from phenanthrene toxicity was most prominently observed when CB or MWCNTs  
199 were present at concentrations of 200  $\mu\text{g/ml}$  or greater (20x mass ratio excess with respect to  
200 phenanthrene). At this MWCNT loading in ZFE media, only infrequent, minor changes in ZFE  
201 morphological phenotypes due to phenanthrene exposure were noted (data not shown, ~5% of  
202 surviving embryos exhibited tail malformations representing a score of 1 on a published 4-point  
203 malformation scale<sup>21</sup> – a incidence we deemed as insignificant to the study’s conclusions), with  
204 no significant differences in embryo survival rates relative to untreated controls (see Figure 3).  
205 However, at reduced carbon nanomaterial loadings of 50  $\mu\text{g/ml}$  or 25  $\mu\text{g/ml}$  in cultures, minor  
206 ZFE phenotypic abnormalities were common with significant decreases in ZFE survival (Figure  
207 3). These abnormalities included enlarged pericardial sac, malformed yolk sac, and shortened  
208 tail, but these defects were associated with nearly complete embryo mortality.<sup>22</sup> Occasional ZFE  
209 survival was noted in 10  $\mu\text{g/ml}$  phenanthrene at a threshold dose of 25  $\mu\text{g/ml}$  of CB and  
210 MWCNTs (Figure 3). Further, 50% ZFE rescue from phenanthrene (10  $\mu\text{g/ml}$ ) toxicity  
211 corresponds to respective additions of 81.3  $\mu\text{g/ml}$  MWCNTs or 81.5  $\mu\text{g/ml}$  CB. Correlation of

212 these results with the Figure 2 adsorption isotherm facilitated determination of the phenanthrene  
213 LD<sub>50</sub> for ZFEs. Given that 50% of the ZFEs survived in 10 µg/ml phenanthrene with a MWCNT  
214 concentration of 81.3 µg/ml, the LD<sub>50</sub> of phenanthrene should correlate with the unadsorbed  
215 concentration of phenanthrene at this same MWCNT concentration of 81.3 µg/ml. Based on this  
216 assessment, the phenanthrene LD<sub>50</sub> for 3-4 hpf ZFEs is determined to be 2.42 µg/ml.

217  
218 No significant differences were noted between MWCNTs and CB ZFE rescue efficacies (i.e.,  
219 same nanomaterials dosing for each rescued LD<sub>50</sub>). However, the duration of ZFE exposure to  
220 phenanthrene prior to exposure to carbon nanomaterial addition to cultures discriminates the two  
221 carbon nanomaterial treatment conditions. Adding CB (200 µg/ml) two hours post-phenanthrene  
222 exposure to ZFEs provides significant rescue effects (80% ZFE survival) while an equal  
223 concentration of MWCNTs added after the same PAH exposure time yields only 30% ZFE  
224 survival (see Figure 4).

225

## 226 Discussion

227 This study assessed the toxicity of the model PAH, phenanthrene, on the ZFE whole organism  
228 culture model, and ZFE toxicity rescue resulting from additions of carbon nanomaterials, CB and  
229 MWCNT, as known sorbent phases shown to remove the model PAH, phenanthrene, from ZFE  
230 solution. Phenanthrene is a known toxin with reported toxicities in *Danio rerio* reporting an LD<sub>50</sub>  
231 of 0.293 µg/ml when exposed to adult fish for 14 days.<sup>23</sup> Despite limited aqueous solubility (1.28  
232 µg/ml),<sup>23</sup> phenanthrene as a model PAH exhibits profound ZFE toxicities in their aqueous culture  
233 model at 10 µg/ml. However, its aqueous toxicity to ZFEs as a model whole organism can be  
234 modulated by adding carbon nanomaterials to ZFE cultures. This modulation is correlated with  
235 nanomaterial adsorption of PAHs, removing PAHs from solution to mitigate intrinsic ZFE toxicity.  
236 MWCNT or CB material addition alone to ZFE cultures did not produce observed toxicity at levels  
237 up to 10 000 µg/ml. A clear trend relates ZFE survival to CB or MWCNT dosing in the presence

238 of phenanthrene, regardless of carbon nanomaterial physical structure. Higher concentrations of  
239 CB or MWCNTs promote ZFE survival in the presence of phenanthrene, demonstrating the  
240 interaction of carbon nanomaterials with phenanthrene in ZFE media to remove PAH toxicity.  
241 Important to the study design, aqueous 1% DMSO media was employed versus ZFE E3 embryo  
242 medium to minimize carbon nanomaterial aggregation: media ionic strength can prompt  
243 increased nanomaterial aggregation. No significant toxicity differences were observed for ZFEs  
244 in 1% DMSO/water over that in E3 ZFE medium.

245  
246 Phenanthrene has four distinct characteristic optical absorption peaks between 250 and 291  
247 nm,<sup>24</sup> allowing spectrophotometric detection of phenanthrene in 1% DMSO solution. Optical  
248 absorbance measurements using the 251nm primary absorption peak characteristic of the  
249 phenanthrene/MWCNT solution were converted to phenanthrene concentration using an  
250 extinction coefficient of  $6.31 \times 10^4$ ,<sup>24</sup> In the absence of MWCNTs, the baseline optical absorbance  
251 for 10 µg/ml phenanthrene was elevated for all wavelengths above its characteristic absorbance  
252 bands due to light scattering of colloidal phenanthrene aggregates ( $\lambda > 300$ nm, Figure 4). This  
253 suggests that the 10 µg/ml phenanthrene aqueous preparation is likely a biphasic system  
254 comprising both dissolved phenanthrene and suspended insoluble phenanthrene aggregate  
255 particles.<sup>25</sup> This is supported qualitatively by an observed visual increase in solution opacity  
256 when phenanthrene in DMSO is added to water. Additionally, the solubility of phenanthrene in  
257 water has been reported to be 1.28 µg/ml,<sup>23</sup> suggesting that a majority of phenanthrene in the 10  
258 µg/ml solutions is suspended as a dispersion. Reductions in solution fluorescence over time  
259 noted in HPLC experimental data also support this conclusion. This system could have been  
260 simplified to homogeneous solutions by reducing phenanthrene concentrations; however,  
261 phenanthrene is not reliably toxic to ZFEs at these lower concentrations where it is readily water-  
262 soluble. Additionally, measuring lower concentrations of MWCNTs can be problematic due to  
263 their tendency to aggregate in solution, leading to imprecise addition of MWCNT masses as

264 volumetric suspensions to the samples (i.e., for any two 25  $\mu$ l MWCNT aqueous dispersed  
265 samples, one may have a different MWCNT mass from the other due to aggregation). The  
266 consequence of both of these issues is that studying the full range of soluble phenanthrene  
267 concentrations causing ZFE toxicity across the entire range of carbon nanophase surface areas  
268 is neither readily nor reliably achieved.

269  
270 Phenanthrene adsorption to MWCNTs is rapid: UV measurements taken within 30 minutes of  
271 addition of MWCNTs to phenanthrene solutions demonstrated a MWCNT concentration-  
272 dependent depletion in both baseline and characteristic phenanthrene optical absorbance (Figure  
273 1). As seen in Figure 2, the good adsorption isotherm fit suggests that a concentration of 50  
274  $\mu$ g/ml MWCNTs adsorbs 56.1% of available phenanthrene at 10  $\mu$ g/ml (Table 1). When  
275 MWCNTs in 1% DMSO were dosed to ZFEs, no intrinsic MWCNT toxic effects were observed.  
276 This is attributed both to the tightly MWCNT-adsorbed species (and their low aqueous solubility  
277 prompting this partitioning to MWCNT surfaces) and to poor organismal access due to MWCNTs  
278 and their aggregates in ZFE media.

279  
280 This supports the hypothesis underlying this research that MWCNT-mediated PAH adsorption for  
281 both the suspended and dissolved phenanthrene phases is responsible for the observed ZFE  
282 viability rescue effects in ZFE cultures. It is important to note that in an environmental scenario,  
283 many endogenous aqueous compounds can compete for available surface adsorption sites on  
284 carbon nanomaterials. Surface-active molecules such as humic acids and other biosurfactants  
285 and polyaromatic species will compete with PAHs for adsorption sites on MWCNTs and CB,  
286 reducing MWCNT-based organism rescue abilities against water-based toxins.<sup>26</sup>

287  
288 Together, these data suggest that irreversible ZFE toxicity occurs following just over 2 hours of  
289 phenanthrene exposure starting at 3-4 hpf ZFEs. Moreover, these data also suggest that CB is

290 able to deplete phenanthrene from the ZFE media more quickly and effectively than MWCNTs for  
291 the observed ZFE protective effect. This difference is attributed to direct carbon nanomaterial-  
292 phenanthrene adsorption differences in media that make this PAH unavailable to the ZFE  
293 cultures – the mechanism proposed for the observed ZFE toxicity rescue. Differences in  
294 phenanthrene adsorption amounts and kinetics by these carbon nanomaterials may arise from  
295 the higher CB surface area as well as different carbon surface structures and their respective  
296 intrinsic sorbate thermodynamics for adsorbing phenanthrene. Alternatively, differences may be  
297 due to different carbon nanoparticle dispersion physical states in the aqueous media exposed to  
298 phenanthrene. CB was observed to disperse more homogeneously in 1% DMSO solutions than  
299 MWCNTs at all solid loadings used, suggesting that this physical aqueous dispersion is an  
300 additional cause for the observed significant differences in ZFE survival rates by providing  
301 different phenanthrene access to each carbon nanomaterial surface in partitioning and adsorption  
302 from the media<sup>27, 28</sup>

303  
304 These data also support tight binding of phenanthrene to both CB and MWCNT nanomaterials in  
305 aqueous dispersions, not easily desorbed into solution. Previous data concluded that adsorption  
306 hysteresis was not observed for phenanthrene and MWCNTs in water.<sup>7</sup> Conversely, the ZFE  
307 rescue effect observed here, and associated decrease in visible phenanthrene concentration  
308 measured by UV/Vis (Figure 1) suggest that irreversible hysteresis may indeed be real. It is also  
309 possible that hysteresis does occur in this case, but at the time of phenanthrene desorption, ZFEs  
310 may have reached a developmental maturity more resistant to its toxicity. The increased rescue  
311 effect observed for CB dosed at 2 hours post-phenanthrene exposure is consistent with the  
312 increased BET surface area of CB relative to MWCNTs. Additionally, another recent report also  
313 confirmed that activated carbon exhibited higher PAH adsorption in aqueous media than  
314 MWCNTs.<sup>5</sup>

315

316 According to Table 1 and Figure 3, fractional adsorption of phenanthrene to MWCNT correlates  
317 well with in vivo data for ZFE survival, reflecting the amounts of phenanthrene not available to  
318 ZFEs in the presence of MWCNTs. The high standard deviations observed for 100, 150, and 200  
319  $\mu\text{g/ml}$  MWCNT concentrations is likely due to MWCNT aggregation, blocking potential adsorption  
320 sites and possibly resulting in non-uniform mass/volume additions of MWCNTs from the 2 mg/ml  
321 MWCNT stock solution to create each isotherm. For comparison, theoretical total surface area of  
322 dissolved phenanthrene at a concentration of 10  $\mu\text{g/ml}$  was estimated using the assumptions that  
323 each molecule has a molecular diameter of 0.79 nm<sup>29</sup> and a maximum close-packed fraction of  
324 surface area occupied by spherical molecules of 0.74. Given these parameters, complete  
325 adsorption of 10  $\mu\text{g/ml}$  of phenanthrene would be expected to require a total MWCNT adsorbed  
326 surface area of 0.0166 m<sup>2</sup>/ml from this solution. For comparison, respective total surface areas  
327 for CB and MWCNTs at concentrations of 100  $\mu\text{g/ml}$  were calculated to be 0.0172 m<sup>2</sup>/ml and  
328 0.0103 m<sup>2</sup>/ml, respectively. For CB, this concentration and adsorption capacity would  
329 theoretically accommodate adsorption of ~104% of all phenanthrene molecules in the 10  $\mu\text{g/ml}$   
330 solution. The observed 70% ZFE survival rate with CB rescue is therefore less than that  
331 predicted by this 100% non-bioavailable theoretical adsorption value. However, multiple factors  
332 influence nanomaterial adsorption capacity in actual ZFE settings, including nanomaterials  
333 aggregation, PAH adsorption/desorption deviation from Langmuir isotherm models, including  
334 reported PAH multilayers<sup>30</sup> and desorption hysteresis<sup>7</sup>. The collective BET-determined surface  
335 area from MWCNT addition is theoretically sufficient to bind 62% of the phenanthrene in this  
336 system, correlating well with the observed ZFE rescue of 60% at this concentration. Actual  
337 phenanthrene adsorption from 1% DMSO Millipore water aqueous solutions, however, shows  
338 higher phenanthrene adsorption (87.5%, Table 1, Figure 2) than these theoretically predicted  
339 MWCNT values.  
340

341 Adsorption of various organic compounds to MWCNTs, including phenanthrene, has also been  
342 previously described by Langmuir models.<sup>31, 32</sup> Phenanthrene adsorption to MWCNTs here fits  
343 moderately well to a Langmuir equation consistent with its fit to a previous Langmuir adsorption  
344 isotherm.<sup>33</sup> The  $R^2$  value correlating these data with the Langmuir model (0.957) is likely reduced  
345 by MWCNT aggregation in solution. Aggregation at higher MWCNT concentrations in water will  
346 reduce their PAH adsorption capacity, deviating from model Langmuir adsorption. Despite this,  
347 the theoretical phenanthrene adsorption capacity of 137 mg/g shown here is higher than that  
348 reported for previous MWCNT data.<sup>33</sup> Previous adsorption capacities of MWCNTs and  
349 phenanthrene reported a  $Q^0$  value of 41.7 mg/g.<sup>33, 34</sup> However, the surface area of the MWCNTs  
350 were reported to be lower and phenanthrene was added in methanol rather than DMSO in these  
351 studies, which could account for the discrepancy.

352  
353 Activated charcoal has been used historically to remove toxins by solution adsorption<sup>35,</sup>  
354 <sup>36</sup> and has shown efficacy even added 1.5 hours after exposure to known toxins.<sup>37</sup> With the 3-4  
355 hpF ZFEs used in this experiment, ZFE death typically occurred within 6 hours of phenanthrene  
356 introduction in control studies. Thus, carbon nanomaterials were needed to provide ZFE rescue  
357 within a few hours of PAH exposure: 2 hours was the latest point producing any significant ZFE  
358 rescue effect. Significant differences in this ZFE rescue effect from phenanthrene toxicity were  
359 observed with CB additions, but not with MWCNT additions (both relative to phenanthrene-only  
360 control). This result correlates well with the higher CB surface area for phenanthrene and its  
361 increasing adsorption capacity for phenanthrene. Importantly, overall results shown are  
362 consistent with previous reports of simple PAH adsorption to MWCNTs in aqueous solutions,<sup>27, 33</sup>  
363 supporting unique, new assertions here that 1) MWCNTs do not cause significant toxicity in  
364 ZFEs, and 2) that MWCNTs have a high adsorptive capacity for PAHs. This is the first report to  
365 correlate this phenanthrene (or any PAH) adsorption with viability influences on living whole  
366 organism cultures such as ZFEs.



367

368 **Conclusions**

369

370 The collective data presented herein demonstrate whole organism viability rescue from  
371 introduced phenanthrene toxicity in ZFE cultures by addition of both CB and MWCNT dispersions  
372 to ZFE aqueous milieu. These carbonaceous nanomaterials dispersions act as sorptive  
373 substrates for rapid phenanthrene removal from ZFE media. The comparatively larger BET  
374 surface area for CB yields greater PAH adsorption capacity for phenanthrene in time-dependent  
375 carbon nanomaterials rescue assays, but does not significantly increase ZFE viability in  
376 concentration-dependent rescue experiments. These results establish that carbon nanomaterial  
377 phases: 1) act as significant sorbent phases for adsorption of sparingly soluble or hydrophobic  
378 compounds from aqueous media, 2) rescue ZFEs from aqueous toxicity from added known toxins  
379 and 3) do not readily release adsorbed adventitious PAH contaminants known to reside on  
380 MWCNTs and CBs from their commercial production into these solutions. Hence, possible  
381 toxicities due to desorption of adventitious adsorbed PAH compounds might not necessarily occur  
382 from carbon nanomaterials in certain aqueous conditions. Also, in the manufacturing of  
383 MWCNTs, it may not be always necessary to completely remove certain tightly adsorbed PAHs  
384 present after synthesis as these compounds may be unlikely to leach or cause significant toxicity  
385 in such assays. Future studies should determine if MWCNT-resident PAHs are more likely to  
386 desorb in more hydrophobic environments in physiological systems, such as partitioning into  
387 adipose tissues, fatty tissues (e.g., brain), cell membranes, hydrophobic pockets of abundant  
388 globular plasma proteins like albumin, or lipid aggregates like lipoproteins or chylomicrons.

389

390 **Acknowledgements.** The authors acknowledge support from a University of Utah SEED grant  
391 (DWG) and University UROP support (to SL).

392

393  
394  
395  
396  
397  
398  
399  
400  
401  
402  
403  
404  
405  
406  
407  
408  
409  
410  
411  
412  
413  
414  
415  
416  
417  
418  
419  
420  
421  
422  
423  
424  
425  
426  
427  
428  
429  
430  
431  
432  
433  
434  
435  
436  
437  
438

## References

1. Rakov, E.G. Carbon nanotubes in new materials. *Russian Chemical Reviews* **82**, 27 (2013).
2. Poland, C.A. et al. Carbon nanotubes introduced into the abdominal cavity of mice show asbestos-like pathogenicity in a pilot study. *Nature nanotechnology* **3**, 423-428 (2008).
3. Monteiro-Riviere, N.A., Nemanich, R.J., Inman, A.O., Wang, Y.Y. & Riviere, J.E. Multi-walled carbon nanotube interactions with human epidermal keratinocytes. *Toxicology letters* **155**, 377-384 (2005).
4. Bacsa, R. et al. High specific surface area carbon nanotubes from catalytic chemical vapor deposition process. *Chemical Physics Letters* **323**, 566-571 (2000).
5. Brooks, A., Lim, H. & Kilduff, J.E. Adsorption uptake of synthetic organic chemicals by carbon nanotubes and activated carbons. *Nanotechnology* **23**, 294008 (2012).
6. Grainger, D.W. & Castner, D.G. Nanobiomaterials and nanoanalysis: opportunities for improving the science to benefit biomedical technologies. *Advanced Materials* **20**, 867-877 (2008).
7. Yang, K. & Xing, B. Desorption of polycyclic aromatic hydrocarbons from carbon nanomaterials in water. *Environmental Pollution* **145**, 529-537 (2007).
8. Jones, C.F. & Grainger, D.W. *In vitro* assessments of nanomaterial toxicity. *Advanced Drug Delivery Reviews* **61**, 438-456 (2009).
9. Keiluweit, M. & Kleber, M. Molecular-level interactions in soils and sediments: the role of aromatic  $\pi$ -systems. *Environmental science & technology* **43**, 3421-3429 (2009).
10. Hill, A.J., Teraoka, H., Heideman, W. & Peterson, R.E. Zebrafish as a model vertebrate for investigating chemical toxicity. *Toxicological Sciences* **86**, 6-19 (2005).
11. Usenko, C.Y., Harper, S.L. & Tanguay, R.L. *In vivo* evaluation of carbon fullerene toxicity using embryonic zebrafish. *Carbon* **45**, 1891-1898 (2007).
12. Király, Z. et al. Selective sorption of phenol and related compounds from aqueous solutions onto graphitized carbon black. Adsorption and flow microcalorimetric studies. *Langmuir* **12**, 423-430 (1996).
13. Westerfield, M. The zebrafish book. (Univ. of Oregon Pr., 2000).
14. Ali, S., van Mil, H.G.J. & Richardson, M.K. Large-scale assessment of the zebrafish embryo as a possible predictive model in toxicity testing. *PloS one* **6**, e21076 (2011).
15. Li, S., Wu, Y. & Whitty, K.J. Ash deposition behavior during char– slag transition under simulated gasification conditions. *Energy & Fuels* **24**, 1868-1876 (2010).
16. Liu, Y. et al. Debundling of single-walled carbon nanotubes by using natural polyelectrolytes. *Nanotechnology* **18**, 365702 (2007).
17. Peigney, A., Laurent, C., Flahaut, E., Bacsa, R. & Rousset, A. Specific surface area of carbon nanotubes and bundles of carbon nanotubes. *Carbon* **39**, 507-514 (2001).
18. Richard, Q. & Yang, R.T. Carbon nanotubes as superior sorbent for dioxin removal. *Journal of the American Chemical Society* **123**, 2058-2059 (2001).
19. Rodriguez-Reinoso, F., Martin-Martinez, J.M., Prado-Burguete, C. & McEnaney, B. A standard adsorption isotherm for the characterization of activated carbons. *Journal of Physical Chemistry* **91**, 515-516 (1987).

- 439 20. Sager, T.M. & Castranova, V. Surface area of particle administered versus mass in determining the  
440 pulmonary toxicity of ultrafine and fine carbon black: comparison to ultrafine titanium dioxide.  
441 *Part Fibre Toxicol* **6**, 1-11 (2009).
- 442 21. Fako, V.E. & Furgeson, D.Y. Zebrafish as a correlative and predictive model for assessing  
443 biomaterial nanotoxicity. *Advanced drug delivery reviews* **61**, 478-486 (2009).
- 444 22. King-Heiden, T.C. et al. Quantum dot nanotoxicity assessment using the zebrafish embryo.  
445 *Environmental science & technology* **43**, 1605-1611 (2009).
- 446 23. Prosser, C.M., Unger, M.A. & Vogelbein, W.K. Multistressor interactions in the zebrafish (< i>  
447 *Danio rerio*</i>): Concurrent phenanthrene exposure and< i> Mycobacterium marinum</i>  
448 infection. *Aquatic Toxicology* **102**, 177-185 (2011).
- 449 24. Jaffé, H.H. & Orchin, M. Theory and applications of ultraviolet spectroscopy. (1962).
- 450 25. Langergraber, G., Fleischmann, N. & Hofstaedter, F. A multivariate calibration procedure for  
451 UV/VIS spectrometric quantification of organic matter and nitrate in wastewater. *Water Science &*  
452 *Technology* **47**, 63-71 (2003).
- 453 26. Wang, X., Tao, S. & Xing, B. Sorption and competition of aromatic compounds and humic acid on  
454 multiwalled carbon nanotubes. *Environmental science & technology* **43**, 6214-6219 (2009).
- 455 27. Chen, J., Chen, W. & Zhu, D. Adsorption of nonionic aromatic compounds to single-walled carbon  
456 nanotubes: Effects of aqueous solution chemistry. *Environmental science & technology* **42**, 7225-  
457 7230 (2008).
- 458 28. Cheng, J., Flahaut, E. & Cheng, S.H. Effect of carbon nanotubes on developing zebrafish (*Danio*  
459 *rerio*) embryos. *Environmental Toxicology and Chemistry* **26**, 708-716 (2009).
- 460 29. Sawamura, S. Pressure Dependence of the Solubilities of Anthracene and Phenanthrene in Water  
461 at 25° C. *Journal of solution chemistry* **29**, 369-375 (2000).
- 462 30. Pan, B. & Xing, B. Adsorption mechanisms of organic chemicals on carbon nanotubes.  
463 *Environmental science & technology* **42**, 9005-9013 (2008).
- 464 31. Wang, S.G. et al. Adsorption of fulvic acids from aqueous solutions by carbon nanotubes. *Journal*  
465 *of Chemical Technology and Biotechnology* **82**, 698-704 (2007).
- 466 32. Lu, C., Chung, Y.-L. & Chang, K.-F. Adsorption thermodynamic and kinetic studies of  
467 trihalomethanes on multiwalled carbon nanotubes. *Journal of hazardous materials* **138**, 304-310  
468 (2006).
- 469 33. Yang, K., Zhu, L. & Xing, B. Adsorption of polycyclic aromatic hydrocarbons by carbon  
470 nanomaterials. *Environmental science & technology* **40**, 1855-1861 (2006).
- 471 34. Yang, K., Wang, X., Zhu, L. & Xing, B. Competitive sorption of pyrene, phenanthrene, and  
472 naphthalene on multiwalled carbon nanotubes. *Environmental science & technology* **40**, 5804-  
473 5810 (2006).
- 474 35. Dąbrowski, A., Podkościelny, P., Hubicki, Z. & Barczak, M. Adsorption of phenolic compounds by  
475 activated carbon—a critical review. *Chemosphere* **58**, 1049-1070 (2005).
- 476 36. Olson, K.R. Activated charcoal for acute poisoning: one toxicologist's journey. *Journal of Medical*  
477 *Toxicology* **6**, 190-198 (2010).
- 478 37. Curtis, R.A., Barone, J. & Giacona, N. Efficacy of ipecac and activated charcoal/cathartic:  
479 prevention of salicylate absorption in a simulated overdose. *Archives of internal medicine* **144**, 48  
480 (1984).

481

482

483

484 **Figures and figure legends, Table (Falconer et al.):**

485

486 **Table 1: Fractional MWCNT uptake of phenanthrene from a 10  $\mu\text{g/ml}$  phenanthrene**  
 487 **aqueous solution**

Concentration MWCNTs ( $\mu\text{g/ml}$ )	% phenanthrene adsorbed	standard deviation
50	56.2	3.1
100	87.5	24.4
150	92.5	22.8
200	95.0	18.17

491

492

493

494

495

496

497

498

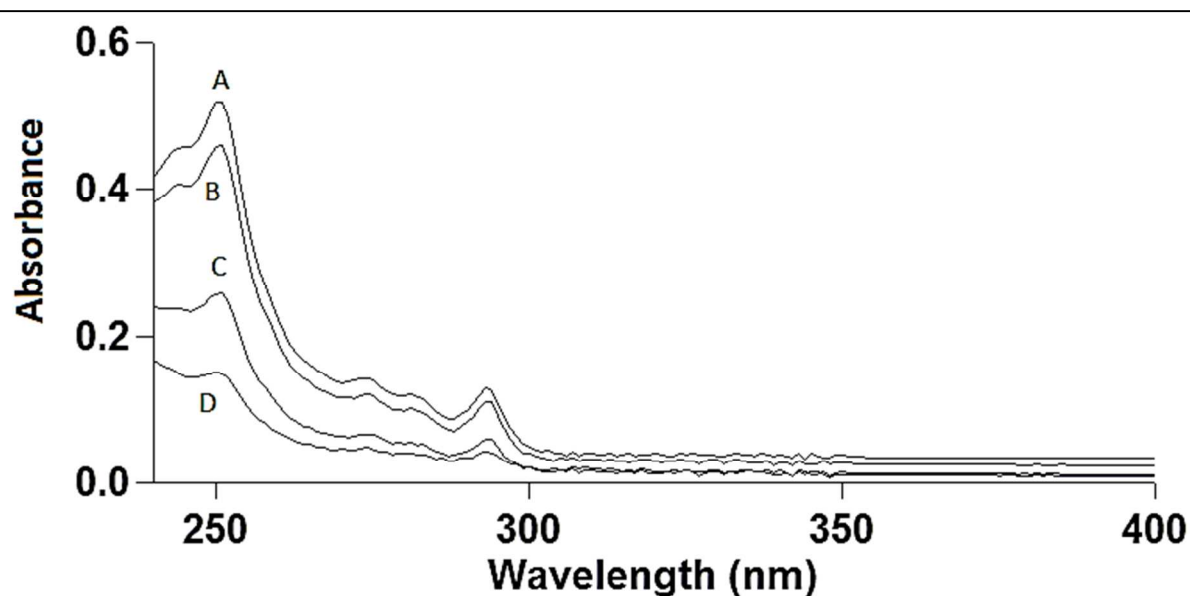
499

500

501

502

503



504 **Figure 1.** Ultraviolet optical absorption spectra of phenanthrene after 40 minutes in 1%  
 505 DMSO aqueous media at room temperature (21°C): (A) 10  $\mu\text{g/ml}$  phenanthrene in 1%  
 506 DMSO; (B) 10  $\mu\text{g/ml}$  phenanthrene in 1% DMSO with 30  $\mu\text{g/ml}$  MWCNT (MWCNT  
 507 separated for UV analysis of supernatant); (C) 10  $\mu\text{g/ml}$  phenanthrene with 100  $\mu\text{g/ml}$   
 508 MWCNT; (D) 10  $\mu\text{g/ml}$  phenanthrene with 200  $\mu\text{g/ml}$  MWCNT (MWCNT separated for UV  
 509 analysis of supernatant).

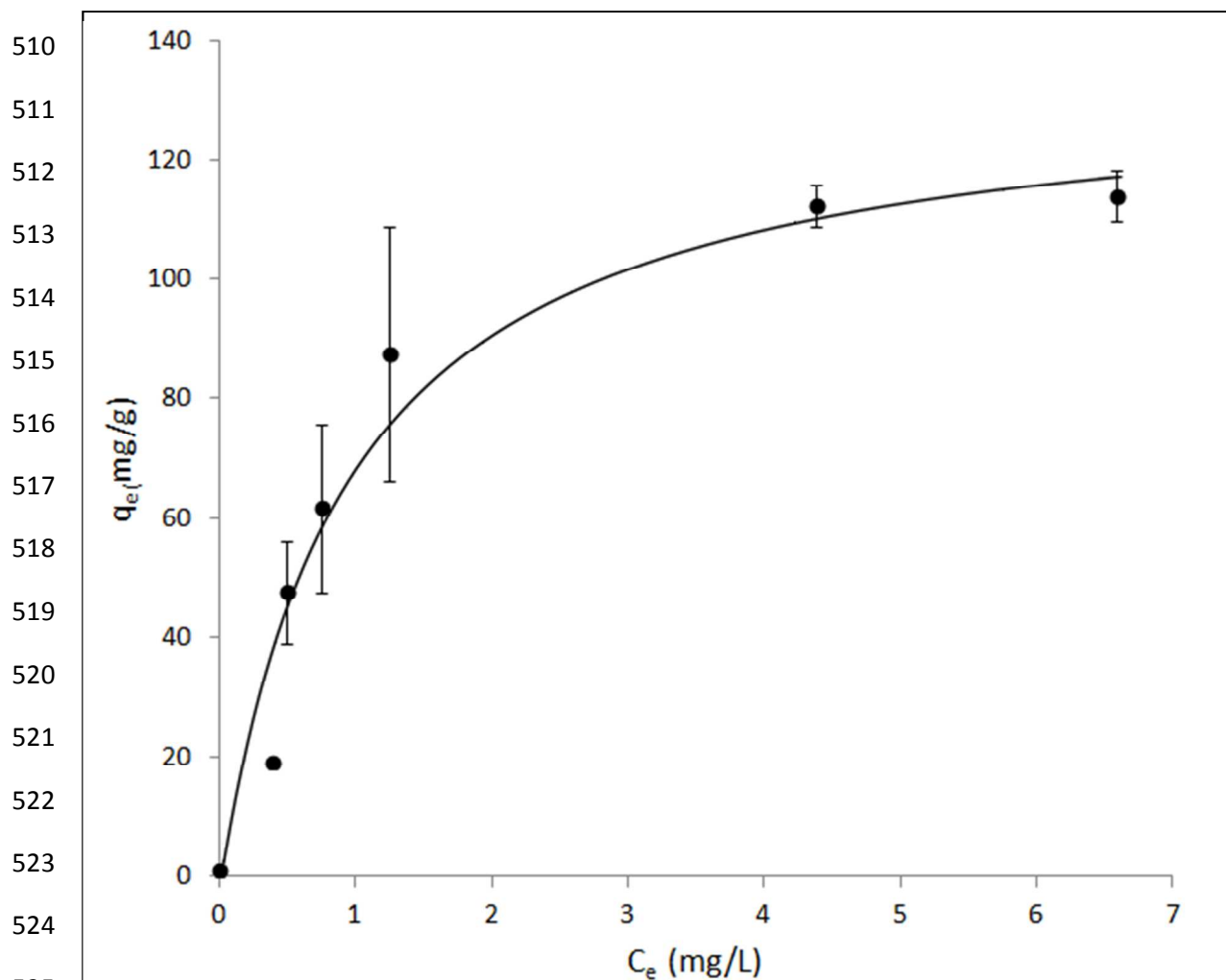


**Figure 2:** Adsorption isotherm for phenanthrene from ASTM research-grade aqueous dispersions onto multi-walled carbon nanotubes at 21°C ( $q_e$ =adsorbed phenanthrene,  $C_e$ =equilibrium concentration).  $R^2 = 0.957$  using the Langmuir adsorption model:  $q_e = Q^0 C_e / (K_d + C_e)$ . A value of  $Q^0 = 137$  for the saturation by phenanthrene is derived from the curve fit and coefficient approximation.

530  
531  
532  
533  
534

535

536

537

538

539

540

541

542

543

544

545

546

547

548

549

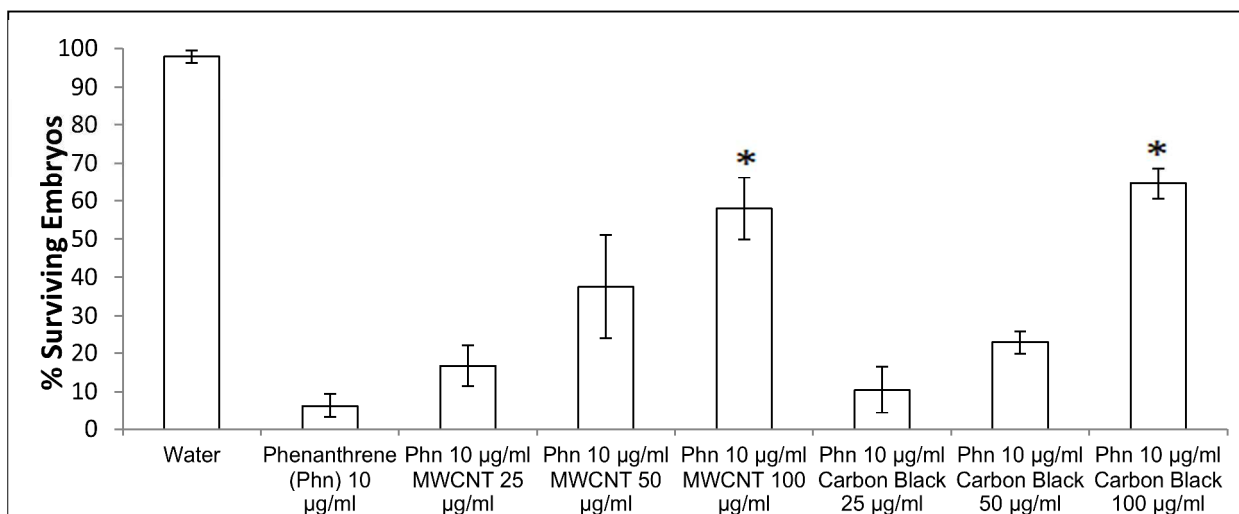


**Figure 3:** Phenanthrene toxicity in zebrafish embryos with various concentrations of either carbon black or MWCNTs added to ZFE media. ZFEs were dosed with phenanthrene at 3–4 hpf and visually assessed for mortality at 4 and 20 hpf. Data represent mean  $\pm$  SE (N=4) and were analyzed by Dunnett's test ( $*p < 0.05$ ). \*represents significant difference from phenanthrene only control (10  $\mu$ g/ml). (Phn=phenanthrene)

550

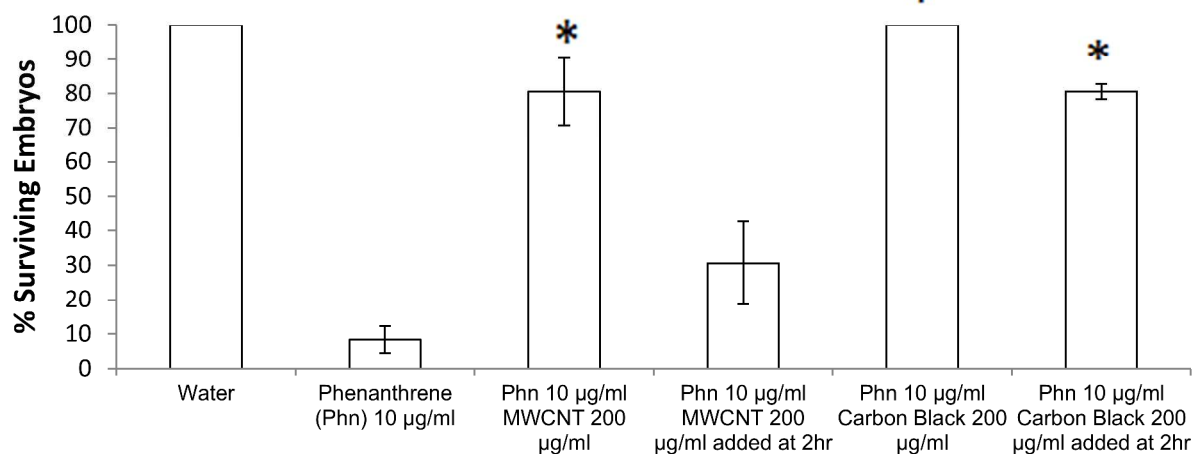


**Figure 4.** Phenanthrene toxicity rescue in ZFEs is observed with MWCNTs or CB added 2 hours after phenanthrene dosing (10  $\mu$ g/ml). Data represent mean  $\pm$  SE (N=3) as analyzed by Dunnett's test ( $*p < 0.05$ ) relative to phenanthrene-only survival controls shown. \*represents significant difference from phenanthrene only (10  $\mu$ g/ml). (Phn=phenanthrene)